

Machine-Learning Based Selection and Synthesis of Candidate Metal-Insulator Transition Metal Oxides

Alexandru B. Georgescu,^{*,†} Peiwen Ren,[‡] Christopher Karpovich,[¶] Elsa
Olivetti,[¶] and James M. Rondinelli^{*,‡}

[†]*Department of Chemistry, 800 East Kirkwood Avenue, Indiana University, Bloomington,
Indiana 47405, United States*

[‡]*Department of Materials Science and Engineering, Northwestern University, Evanston, IL
60208, USA*

[¶]*Department of Materials Science and Engineering, Massachusetts Institute of Technology,
Cambridge, MA 02139 USA*

E-mail: georgesc@iu.edu; jrondinelli@northwestern.edu

Abstract

The discovery of materials that exhibit a metal-insulator transition (MIT) is key to the development of multiple types of novel efficient microelectronic and optoelectronic devices. However, identifying MIT materials is challenging due to a combination of high computational cost of electronic structure calculations needed to understand their mechanism, the mechanisms' complexity, and the labor-intensive experimental validation process. To that end, we use a machine learning classification model to rapidly screen a high-throughput crystal structure database to identify candidate compounds exhibiting thermally-driven MITs. We focus on three candidate

oxides, $\text{Ca}_2\text{Fe}_3\text{O}_8$, CaCo_2O_4 , and CaMn_2O_4 , and identify their MIT mechanism using high-fidelity density functional theory calculations. Then, we provide a probabilistic estimate of which synthesis reactions may lead to their realization. Our approach couples physics-informed machine learning, density functional theory calculations, and machine learning-suggested synthesis to reduce the time to discovery and synthesis of new technologically relevant materials.

Introduction

Electronically active correlated electron materials and their properties can be challenging to predict, requiring high-fidelity, resource-intensive calculations to understand their electronic structure, followed by significant time and resource investment for their synthesis, as well as the accurate experimental measurement of their electronic properties. Further, the dependence of the predicted property on the exact electronic structure methodology - which often includes adjustable parameters - , combined with the high time and resource cost of synthesizing a novel material, make the cycle of discovery relatively slow.

This is particularly true for metal-insulator transition (MIT) materials, which undergo a phase transition from a metallic state to an insulating state, or vice versa, through changes in external conditions, such as temperature, pressure, or doping,^{1,2} leading to a wide variety of applications.³⁻⁸ Here, we focus on thermally-driven MITs, as the state of these materials usually can be switched not just by temperature, but also with an applied electric field, mechanical stress, or light, a group with strong potential technological interest - however, there are only under 70 stoichiometrically distinct materials that display this property, which we have previously provided a database for⁹.

Despite the same macroscopic outcome - a change in electrical resistivity with temperature - the mechanisms, the stoichiometry, and the crystal structure of these materials are often dissimilar, and their interplay is often the subject of debate - and often the exact mechanism is the subject of debate. The transition from the metallic phase to the insulating phase

is usually triggered by a coupled change in symmetry in both the electronic phase and in crystal structure, which is often difficult to decouple experimentally and theoretically; however recent experiments have made progress using for example isotope effects¹⁰ and superlattice structures¹¹⁻¹⁴. Theoretical methods to simulate the ground state show dependence on the computational methodology, making the prediction of new compounds difficult;¹⁵⁻¹⁹ complexities associated with doping and vacancies can often further complicate the picture²⁰⁻²². The temperature dependence of the transition poses an additional challenge, as density functional theory (DFT) is a ground state (T=0K) theory. While a zero temperature calculation may help elucidate the nature of the insulating ground state, it is difficult to predict with high accuracy whether a metal-insulator transition will occur with temperature. As a result, much of the focus in the literature has been on explaining the difference between the two states for previously experimentally observed MITs. Even though computational models have so far been able to reproduce varying aspects of the metal-insulator transition, and the temperature dependence of the electronic¹⁸ or structural degrees of freedom²³, this has always been done on materials with a previously experimentally confirmed metal-insulator transition, and at high computational expense, and is at this point not feasible in a high throughput way. Finally, these calculations do not provide guidance on how to synthesize a new material after its prediction.

Machine learning tools are increasingly used to understand and discover materials, to process - and find patterns - both in theoretical and in experimental data²⁴⁻²⁹, as well as to substitute explicit DFT calculations^{26,30-32}. As machine learning tools become more accurate with larger training datasets, materials discovery becomes more challenging when the number of materials with a given property is limited, as is the case for metal-insulator transition compounds, and quantum materials more broadly. We have previously begun addressing this challenge using a tree-based machine learning model - which requires fewer training examples than neural networks- , with physically informed feature choices.⁹

Here, we use a combination of machine learning (ML) tools and detailed electronic struc-

ture calculations, to identify candidate MIT oxides and their synthesis pathways. We have previously reported a tree-based ML classifier trained on an MIT database and novel features, and now we use it to filter compounds in the high-throughput DFT database Materials Project. We obtain 36 compounds from our filtration, from which we down-select to $\text{Ca}_2\text{Fe}_3\text{O}_8$, CaCo_2O_4 , and CaMn_2O_4 for high-fidelity DFT study. We find that the insulating state of $\text{Ca}_2\text{Fe}_3\text{O}_8$ is driven by a combination of trigonal-symmetry induced orbital order and magnetism, similar to what we’ve recently discussed in the 2D van der Waals dihalides and trihalides (MX_2 and MX_3), as well as in face and edge-connected octahedral perovskites^{33,34}. This ferrite’s ground state displays an unusual 4+ ionization state for the Fe atom, which may nonetheless be stabilized by the material’s trigonal crystal field. CaCo_2O_4 is likely to have a mechanism similar to that of LaCoO_3 ³⁵⁻³⁷ with a low-spin insulating state and a high-spin metallic state, while CaMn_2O_4 may have a magnetically-driven transition. For the Fe and the Mn compounds, we use a non-magnetic calculation as a proxy for the metallic phase. Last, we propose synthesis precursors and possible transitions using natural language processing. These synthesis pathways should lower the time lag between our proposal and possible validation of these materials and their electronic properties.

Methods

Our computational methodology includes multiple steps (Figure 1). The first, which was reported in previous work⁹, is training a tree-based (XGboost) ML-based classifier on a wide variety of materials, consisting of all the known materials with a thermally-driven metal-insulator transition at the time of building the classifier.¹ The second step is to use this tool to scan over a high throughput database of crystal structures, namely Materials Project³⁸, within a range of parameters where we believe that the classifier’s predictions

¹This classifier uses a combination of features that are known from previous work as being key to whether a material is an MIT or not (unscreened Hubbard U, charge transfer energy), structural features related to relevant energy scales (metal-metal, and metal-ligand distances), and other features which were found to be relevant via F1 scores by the classifier model (Global Instability Index, Average Deviation of the Covalent Radius).

are at their most reliable: the materials space scanned should of course include materials not in our dataset, but should not stray too far in order to be reliable. A total of 529 structures were pulled from the MP database. After running these compounds through the MIT binary classifier, 59 structures not in the training set were predicted to exhibit a MIT; as multiple structures are polymorphs of the same stoichiometry, there are only 36 unique chemical formulas as a result of our filtration; these are presented in Table 1, with their respective d-electron count. To interface our classifier with the Materials Project, we use the Pymatgen package to interface with the Materials API.³⁹ There are 3 query parameters: the chemical composition, energy above the convex hull, and the number of atoms in the unit cell. The chemical composition search space is constrained to $A_mB_nX_k$ ternary compounds, with elements A and B as the cations, X as the anion, and m, n, k arbitrary non-zero integers, with $A=\{\text{Ca, Sr, Ba, La}\}$, $B=\{\text{Ti, V, Cr, Mn, Fe, Co, Ni, Cu, Zr, Nb, Mo, Tc, Ru, Rh, Pd, Ag}\}$, and $X = \{\text{N, S, O}\}$. In order to limit ourselves to materials that are possible to synthesize, we limit the search to materials that less than 100 meV per atom above the convex hull.

Next, we curate the identified materials, labeling their current experimental status, and eliminating materials with less than one electron per d-shell (in an ionic model) for the transition metal atoms, namely CaMoN_3 , BaCr_2O_7 , $\text{BaMo}_3\text{O}_{10}$, $\text{BaNb}_4\text{O}_{11}$, CaNb_2O_6 . Finally, we perform density functional theory calculations on the compounds where the experimental status is not known, to assess the possibility of a metal-insulator transition and its mechanism on three compounds, $\text{Ca}_2\text{Fe}_3\text{O}_8$, CaCo_2O_4 and CaMn_2O_4 . We next perform density functional theory calculations using Vienna Ab initio Simulation Package (VASP);^{40–42} unless otherwise mentioned, the SCAN meta-GGA exchange-correlation functional⁴³ is used, which has been proven to give electronically accurate ground states on MIT and correlated insulating materials with 3d-orbital transition metal ions.⁴⁴ To predict hypothetical synthesis parameters for the identified possible MIT compounds, we use ML methods developed in⁴⁵ to predict precursors, synthesis route, and solid-state synthesis temperatures.

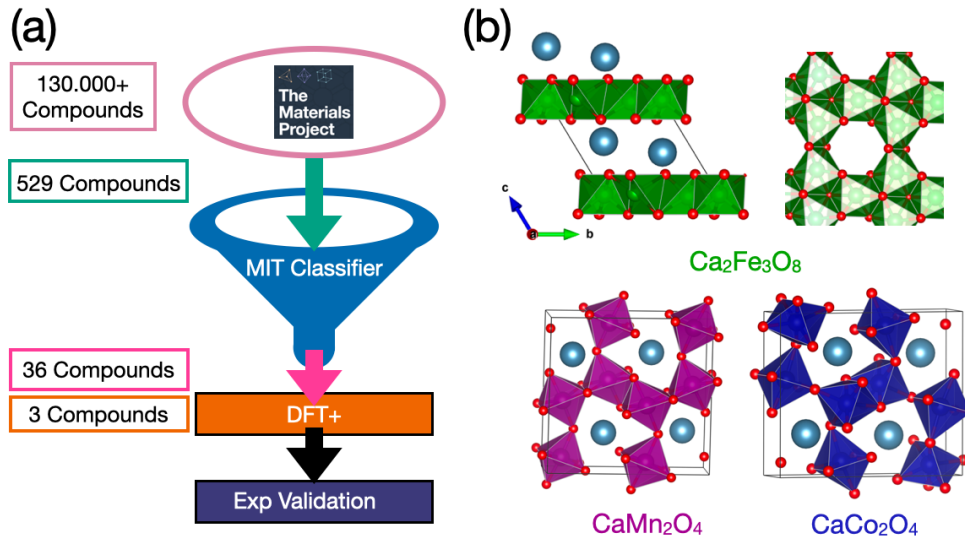


Figure 1: (a) Workflows for MIT materials identification. In this work we’ve performed filtration of materials in the Materials Project, identified a few key materials and performed DFT calculations on them and are proposing them for experimental validation. (b) Crystal structures of the candidate MIT materials. The top right image shows the structure of a single layer of Fe-O polyhedra, which may lead to complex spin structures.

Results and Discussion

We performed DFT calculations using the SCAN functional for CaCo_2O_4 (or $\text{Ca}(\text{CoO}_2)_2$ as given in Table 1). Figure 2 shows the band structure and the density of states (DOS) plots for both the low-spin ($S = 0$) and intermediate-spin ($S = 1$) configurations side by side. The high spin ($S = 2$) state is significantly higher in energy and not shown. Consequences of a Hubbard U correction on the electronic structure are presented in the SI.

The low-spin configuration has a band gap as dictated by the crystal field splitting (band gap of 1.67 eV), while the high-spin structure is metallic; the low-spin structure is the ground state. These results are similar to those of the metal-insulator transition in LaCoO_3 . The Co atoms in CaCo_2O_4 and LaCoO_3 both have a +3 oxidation state, resulting in a d^6 electronic configuration. In LaCoO_3 , as the temperature increases, a superposition of the intermediate and high-spin multiplet states become more populated, closing the band gap. We propose that CaCo_2O_4 will have a similar transition from a non-magnetic insulating state at low temperatures to a metallic state at high temperatures.

Table 1: Table of materials identified by the classifier as possibly displaying an MIT, as sorted by their transition metal d-orbital filling, d^n .

| Compound | d^n | Compound | d^n | Compound | d^n |
|--|-------|---|-------|--|-------|
| CaMn ₄ S ₈ | 1,2 | Ca ₄ Mn ₄ O ₁₁ | 3,4 | Ca ₂ Co ₃ O ₈ | 5 |
| Ca ₂ Cr ₃ O ₈ | 2 | CaMn ₄ O ₈ | 3,4 | Ca ₃ Co ₂ O ₇ | 5 |
| CaCrN ₂ | 2 | LaMn ₂ O ₅ | 3,4 | CaCoO ₃ | 5 |
| CaCr ₄ O ₈ | 2, 3 | BaMn ₃ O ₆ | 3, 4 | CaCo ₂ O ₄ | 6 |
| CaNi ₂ O ₈ | 3 | CaMn ₃ O ₆ | 3, 4 | Ca ₂ Co ₂ O ₅ | 6 |
| Ca ₂ Mn ₃ O ₈ | 3 | Ca ₂ Fe ₃ O ₈ | 4 | Ca ₃ Ni ₂ O ₇ | 6 |
| Ca ₃ Cr ₃ N ₅ | 3 | Ca ₂ Mn ₂ O ₅ | 4 | CaNiO ₃ | 6 |
| CaCr ₂ O ₄ | 3 | Ca ₃ Fe ₂ O ₇ | 4 | BaNi ₄ O ₈ | 6, 5 |
| CaMnO ₃ | 3 | CaMn ₂ O ₄ | 4 | CaNi ₂ O ₄ | 7 |
| BaMn ₆ O ₁₂ | 3, 4 | CaMn ₄ N ₄ | 4, 5 | | |
| BaMn ₄ O ₈ | 3, 4 | BaFe ₄ O ₇ | 5 | | |

The Ca₂Fe₃O₈ polymorph identified by our classifier, (mp-1311759 on Materials Project), is a pseudo-2D material, with Ca ions filling the interstitial space between layers of FeO₆ octahedra. This material is isosymmetric to the binary Mn₅O₈ compound, however its dimensionality is reduced by replacing layers of the Mn ion with Ca.

The 2D layers display a honeycomb lattice structure that strongly suggests the possibility of novel magnetic states, particularly as a result of spin frustration. A detailed study of non-collinear spin structures is beyond the scope of this paper, as we focus on collinear calculations in this work. Here Fe⁴⁺ is in a d^4 electronic configuration, an unusual oxidation state for oxides with octahedral crystal fields. As we have shown in previous work,^{33,34} edge connected octahedra with transition metal ions in a pseudo-2D material lead to an additional, trigonal splitting of the orbitals. In this material, it may provide an additional ligand field stabilization energy, which may be responsible for the material’s relative stability as computed by the materials project (~ 36 meV/atom above the Hull).

By doubling the unit cell to two formula units to allow for anti-ferromagnetic ordering, our calculations predict an anti-ferromagnetic, insulating ground state, while the first excited state predicted is ferromagnetic and metallic - the ground state found on Materials Project. The material might then display a transition to a metallic state both as a function of tem-

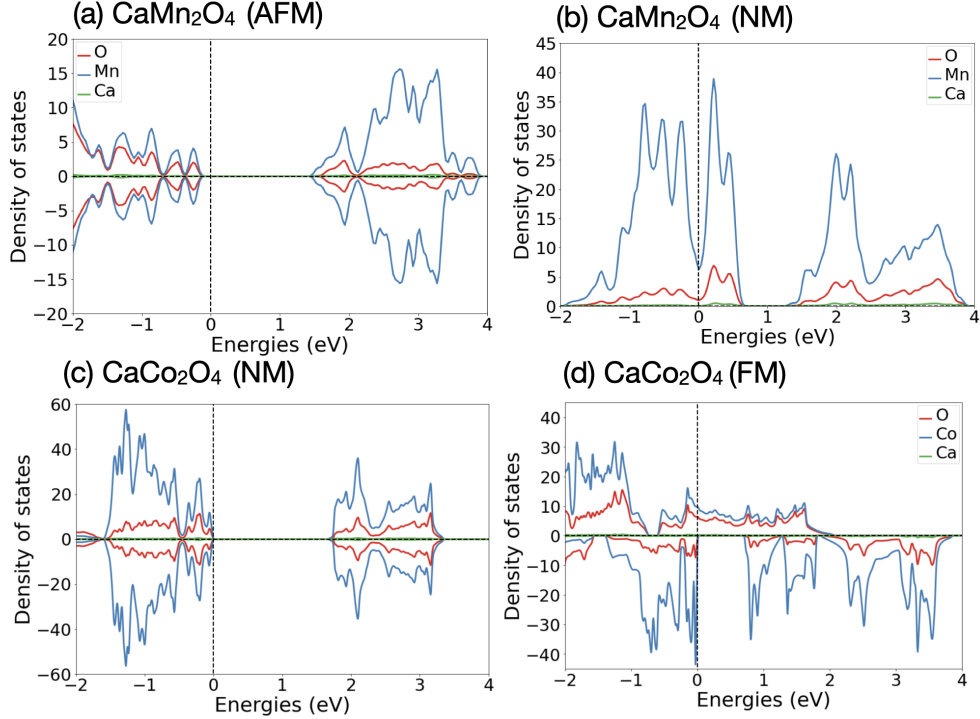


Figure 2: a) and b) Density of states for CaMn_2O_4 suggests the possibility of a magnetism-driven transition. c) and d) Density of states for CaCo_2O_4 in the non-magnetic $S=0$ and FM $S=1$ state, show a similar possible transition mechanism as in LaCoO_3 , with the ground state non-magnetic, and a spin-driven transition as the temperature is raised.

perature, but also as a function of magnetic field, making it a magnetoresistive material. In order to obtain the ground state we've identified, we had to double the unit cell from Materials Project, allowing us to find a magnetic anti-alignment between the layers, while each layer has a non-zero magnetic moment. In the ferromagnetic state, which has the second lowest energy, the material is metallic, pointing to the possibility of controlling its resistivity by applied magnetic field. The magnetic moment of each Fe site in the ground state is $2\mu_B$, an intermediate spin state; the point group symmetry of the atoms is C_{2h} - a symmetry breaking subset of the trigonal symmetry. As discussed in previous work, this then suggests that there is no degeneracy left in the Fe d-basis. The orbital basis then consists of a fully-occupied lowest energy orbital, and two non-degenerate, half-filled, spin-polarized orbitals on each Fe atom. Up to the writing of this paper, this material has not been experimentally observed. Synthesis methods presented in this work may help guide its validation.

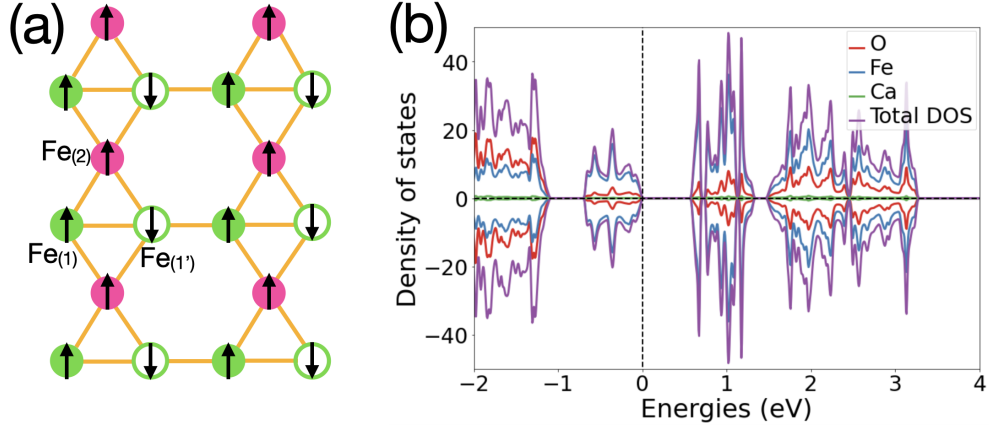


Figure 3: a) The magnetic order for one layer of $\text{Ca}_2\text{Fe}_3\text{O}_8$: all Fe are in a $S=1$ state, the structurally equivalent $\text{Fe}_{(1)}$ and $\text{Fe}_{(1')}$ have different spin orientation, while the $\text{Fe}_{(2)}$ has a different symmetry, but has the same spin state as $\text{Fe}_{(1)}$. The magnetic order breaks the symmetry of the honeycomb, and leads to aligned spin chains within each layer, with non-zero magnetic moment per layer. The magnetic moments of alternating layers cancel out, leaving the material with net zero total magnetization. (b) Projected density of states for the ground state of the material

CaCo_2O_4 exhibits a network of both edge and corner sharing CoO_6 octahedra, with Ca atoms interspersed. Co^{3+} adopts a d^6 electronic configuration. Despite the additional symmetry breaking beyond octahedral due to both corner and edge-connected octahedra, the octahedral crystal field splitting dominates, and we find that the non-magnetic $S = 0$ state, with the three orbitals lowest in energy completely filled, is the ground state. Antiferromagnetic states could not be stabilized in this material, suggesting that they may be unphysical in this material. We were able to stabilize $S = 1$ and $S = 2$ states by enforcing a total magnetization in the material: these states are metallic, and the lowest energy state is still higher in energy than the $S = 0$ state, and metallic - as is the case of LaCoO_3 . The band gap and energy difference between the insulating and metallic states is higher, so it is likely that the electronic transition may be sharper than in LaCoO_3 , and is likely to happen at a higher temperature.

Similar to LaCoO_3 ⁴⁶, this material may have potential applications in microelectronic applications, for example in Resistive RAM memories, and in potential mm radio frequency (mm RF) devices due to its combination of sharp transition, high operating temperature,

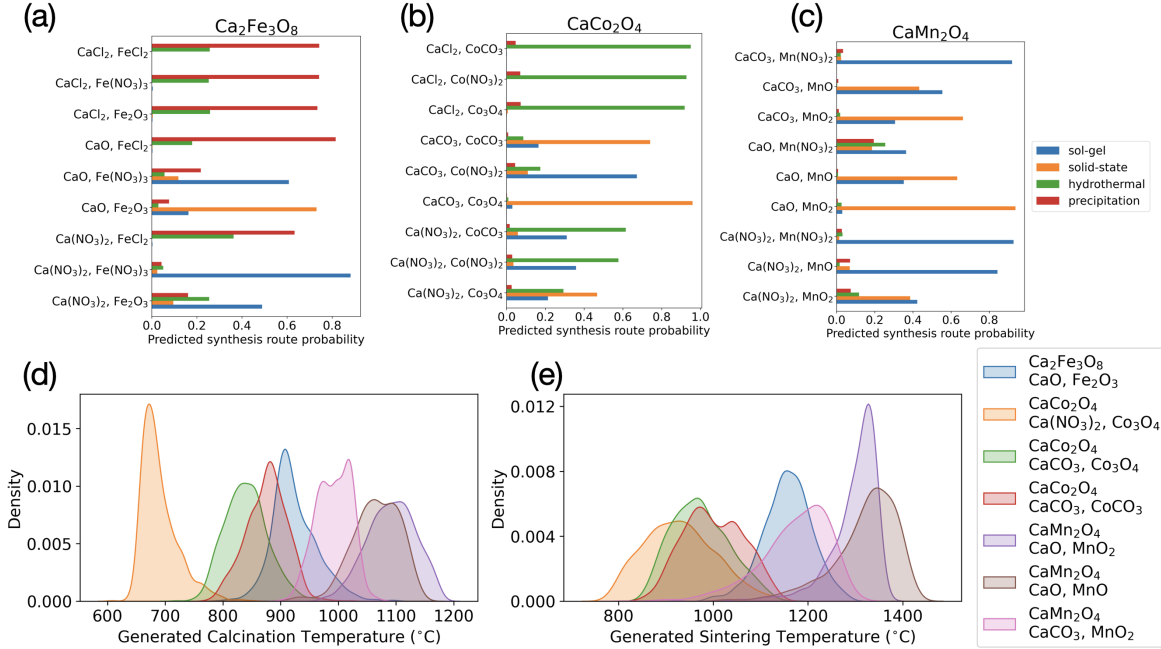


Figure 4: ML-generated synthesis precursor predictions for the 3 compounds discussed in the main text (a,b,c) and predicted calcination (d) and sintering (e) temperatures for their respective predicted solid-state synthesis routes.

and low electric field needed to induce a transition.

In LaCoO_3 , the ground state of the Co d -electrons is the $t_{2g}^6 e_g^0$ low-spin, $S = 0$ configuration. The band gap is determined by the crystal field splitting between the empty e_g and filled t_{2g} states. As the temperature is raised, electrons are excited from the t_{2g} orbitals into the e_g orbitals, leading to a combination of a higher energy $t_{2g}^4 e_g^2$ configuration (high-spin, $S = 2$), and intermediate-spin ($t_{2g}^5 e_g^1$, $S = 1$). The calculations using SCAN show a higher energy difference between the insulating state and the metallic state in the new compound than in LaCoO_3 , so we investigated how this relative energy difference may depend on the particular choice of treatment of the correlated state. To do so, we also performed calculations using the PBE functional with an additional +U correction, in the simplified Dudarev +U formalism, using the Perdew-Burker-Erzenhof (PBE) exchange correlation formalism. Our results suggest the possibility of a sharper metal-insulator transition or a higher transition temperature than that of LaCoO_3 of $T_{MIT} = 600\text{K}$, as well as the possibility that CaCo_2O_4 may always be an insulator.

CaCo₂O₄ has been synthesized in polycrystalline form,⁴⁷ and has not been studied conclusively to exclude potential MIT: the polycrystalline sample did exhibit insulating behavior (ρ) when measured in the temperature (T) range of 10K to 380K, leaving open the possibility of a transition at higher temperature as suggested by our calculations. The material also showed metallic-temperature-dependent large thermoelectric power. The polycrystalline nature of the sample may also contribute to extra resistivity during measurement since charge carriers can scatter off the grain boundaries. This suggests the strong possibility that new measurements on higher quality samples of this material may elaborate further on the promising electronic structure of this material.

Experimentally, this material exhibits a T_N of 240K, however there are no single-crystal measurements of this material’s resistivity. Suppression of magnetic order in this material may lead to a closing of its gap. CaMn₂O₄ crystallizes in the orthorhombic Pbcm space group. Ca²⁺ is bonded in an 8-coordinate geometry to eight O²⁻ atoms. Mn³⁺ is bonded to six O²⁻ atoms, form a mixture of edge and corner-sharing MnO₆ octahedra. We have also performed multiple magnetic calculations, and while our search over possible magnetic order is not exhaustive, the material is insulating even in the ferromagnetic state (which is normally the most likely to be metallic of possible magnetic states). We find that in the non-magnetic state, the material is metallic. We conclude that this material may display an MIT with magnetism playing a key role.

Figure 4 (top) shows the predicted precursors for each compound along with the corresponding probability of a solid-state, sol-gel, hydrothermal, or precipitation synthesis route. For instance, for Ca₂Fe₃O₈ we have 5 precipitation, 3 sol-gel, and 1 solid-state route predicted, for CaCo₂O₄ we have 5 hydrothermal, 3 solid-state, and 1 sol-gel route predicted, and for CaMn₂O₄ we have 6 sol-gel and 3 solid-state routes predicted. Plotting the predicted probabilities allows us to examine what reactions might have more than one viable option. For instance, for the synthesis of CaMn₂O₄ from Ca(NO₃)₂ and MnO₂ we see that sol-gel and solid-state are almost equally likely routes in terms of how promising they are to synthesize

the target compound.

From the predicted synthesis reactions for the MIT compounds, we took the ones which were predicted to be solid-state and predicted appropriate calcination and sintering temperature distributions for the reactions. Figure 4 (bottom) depicts the generated calcination and sintering temperature distributions for the solid-state routes predicted for each of the MIT compounds. Lower processing conditions are desirable in many cases due to energy savings capabilities and manufacturing requirements. We see that the model predicts that for CaCo_2O_4 synthesizing the compound using $\text{Ca}(\text{NO}_3)_2$ and Co_3O_4 would require a much lower calcination temperature than using CaCO_3 and Co_3O_4 or CaCO_3 and CoCO_3 . Similarly, for the synthesis of CaMn_2O_4 , we see that using CaCO_3 and MnO_2 affords a lower predicted calcination temperature range than CaO and MnO_2 or CaO and MnO . Such predictions reveal which reactions are compatible in certain temperature ranges and thus can better inform experimental design.

Conclusions

In this work, we proposed a workflow for the computational prediction of correlated materials that display a metal-insulator transition. Our current work integrated ML tools and DFT, starting with the previously built database and ML classifier, applying it to high-throughput libraries to filter materials, evaluation of possible mechanisms and synthesis of specific materials. Provided experimental validation of one or more of the materials we propose, our materials discovery methodology would rapidly accelerate the discovery of new metal-insulator transition materials - and correlated electron materials more generally. Our tools are readily available online for use by other scientists.

As no reliable quantitative methods of determining suitable reaction conditions exist, our approach could help guide experimentalists with initial suggestions for synthesis precursors, route, and conditions to aid in synthesis planning for the discovery and design of new ma-

terials. We note that we do not perform here DFT calculations to estimate which synthesis method is more likely to lead to the compounds we've predicted: these are unlikely to be reliable without an in-depth study of all the possible factors involved in the synthesis (pH, temperature, aqueous environment⁴⁸).

We note that we have also found that the classifier identifies the brownmillerite $\text{Ca}_2\text{Co}_2\text{O}_5$ as a metal-insulator transition compound: while this material may display an MIT, we find that the complex unit cell required to simulate it realistically, as well as the interplay of polymorphism and magnetic states, make it difficult to study its transition mechanism within the scope of this paper. Nonetheless, this material may display a metal-insulator transition, provided it can be grown as a single phase.

This research was supported in part through the computational resources and staff contributions provided for the Quest high performance computing facility at Northwestern University which is jointly supported by the Office of the Provost, the Office for Research, and Northwestern University Information Technology. The information, data, or work presented herein was funded in part by the Advanced Research Projects Agency-Energy (ARPA-E), U.S. Department of Energy, under Award Number DE-AR0001209 and the National Science Foundation (DMR-2324173). The views and opinions of authors expressed herein do not necessarily state or reflect those of the United States Government or any agency thereof.

Supporting Information Available

The Supporting Information is available free of charge at: [*Link to be inserted*], and relevant structures and the pipeline used to identify them can be found at:

<https://github.com/alexandrub53/MachineLearning-MetalInsulator>

Information includes

1. Comparison of CaCo_2O_4 and LaCoO_3 energy differences between $S=0$ and $S=1$ states for varying U

2. Relative energies for different magnetic configurations for $\text{Ca}_2\text{Fe}_3\text{O}_8$ and CaMn_2O_4
3. Additionally, the GitHub repository contains the scripts used to identify the materials identified in this paper, and optimized crystal structures for the three compounds studied.

References

- (1) Shao, Z.; Cao, X.; Luo, H.; Jin, P. Recent progress in the phase-transition mechanism and modulation of vanadium dioxide materials. *NPG Asia Materials* **2018**, *10*, 581–605.
- (2) Kisiel, E.; Salev, P.; Poudyal, I.; Baptista, F.; Rodolakis, F.; Zhang, Z.; Shpyrko, O.; Schuller, I. K.; Islam, Z.; Frano, A. High-Resolution Full-field Structural Microscopy of the Voltage Induced Filament Formation in Neuromorphic Devices. 2023.
- (3) Lee, Y. J.; Kim, Y.; Gim, H.; Hong, K.; Jang, H. W. Nanoelectronics Using Metal-Insulator Transition. *Advanced Materials* 2305353.
- (4) Qiu, E.; Zhang, Y.-H.; Ventra, M. D.; Schuller, I. K. Reconfigurable Cascaded Thermal Neuristors for Neuromorphic Computing. *Advanced Materials* 2306818.
- (5) Chen, L.; Chen, S.; Cui, Y.; Luo, H.; Gao, Y. Modulation of the metal-insulator transition in VO_2 nanoparticles with $n\text{Ru}+\text{W}$ ($n=1-4$) codoping: Implications for energy-saving smart windows. *Vacuum* **2022**, *201*, 111079.
- (6) Cui, Y.; Ke, Y.; Liu, C.; Chen, Z.; Wang, N.; Zhang, L.; Zhou, Y.; Wang, S.; Gao, Y.; Long, Y. Thermochromic VO_2 for Energy-Efficient Smart Windows. *Joule* **2018**, *2*, 1707–1746.
- (7) Hoffmann, A. et al. Quantum materials for energy-efficient neuromorphic computing: Opportunities and challenges. *APL Materials* **2022**, *10*.

- (8) Schofield, P.; Bradicich, A.; Gurrola, R. M.; Zhang, Y.; Brown, T. D.; Pharr, M.; Shamberger, P. J.; Banerjee, S. Harnessing the Metal–Insulator Transition of VO₂ in Neuromorphic Computing. *Advanced Materials* **2023**, *35*, 2205294.
- (9) B. Georgescu, A.; Ren, P.; R. Toland, A.; Zhang, S.; D. Miller, K.; W. Apley, D.; A. Olivetti, E.; Wagner, N.; M. Rondinelli, J. Database, Features, and Machine Learning Model to Identify Thermally Driven Metal–Insulator Transition Compounds. *Chemistry of Materials* **2021**, *33*, 5591–5605.
- (10) Rischau, C. W.; He, X.; Mazza, G.; Gariglio, S.; Triscone, J.-M.; Ghosez, P.; del Valle, J. Oxygen isotope effect in $\{\mathrm{VO}\}_2$. *Phys. Rev. B* **2023**, *107*, 115139.
- (11) Varbaro, L.; Mundet, B.; Dominguez, C.; Fowlie, J.; Georgescu, A. B.; Korosec, L.; Alexander, D. T. L.; Triscone, J.-M. Electronic Coupling of Metal-to-Insulator Transitions in Nickelate-Based Heterostructures. *Advanced Electronic Materials* **2023**, *9*, 2201291.
- (12) Navarro, H.; Das, S.; Torres, F.; Basak, R.; Qiu, E.; Vargas, N. M.; Lapa, P. N.; Schuller, I. K.; Frano, A. Disentangling transport mechanisms in a correlated oxide by photoinduced charge injection. *Phys. Rev. Mater.* **2023**, *7*, L123201.
- (13) Majhi, P.; Mitra, S.; Singh, A.; Ghosh, B.; Reddy, V. R.; Saha, S.; Raychaudhuri, A. K. Phase coexistence and resistance relaxation kinetics in NdNiO₃ films below the metal-insulator transition temperature. *Phys. Rev. B* **2023**, *108*, 064103.
- (14) Domínguez, C.; Fowlie, J.; Georgescu, A. B.; Mundet, B.; Jaouen, N.; Viret, M.; Suter, A.; Millis, A. J.; Salman, Z.; Prokscha, T.; Gibert, M.; Triscone, J.-M. Coupling of magnetic phases at nickelate interfaces. *Phys. Rev. Mater.* **2023**, *7*, 065002.
- (15) Liang, Y. G.; Lee, S.; Yu, H. S.; Zhang, H. R.; Liang, Y. J.; Zavalij, P. Y.; Chen, X.; James, R. D.; Bendersky, L. A.; Davydov, A. V.; Zhang, X. H.; Takeuchi, I. Tuning the

- hysteresis of a metal-insulator transition via lattice compatibility. *Nature Communications* **2020**, *11*, 3539.
- (16) Meyers, D.; Liu, J.; Freeland, J. W.; Middey, S.; Kareev, M.; Kwon, J.; Zuo, J. M.; Chuang, Y.-D.; Kim, J. W.; Ryan, P. J.; Chakhalian, J. Pure electronic metal-insulator transition at the interface of complex oxides. *Scientific Reports* **2016**, *6*, 27934.
- (17) Han, Q.; Millis, A. Lattice Energetics and Correlation-Driven Metal-Insulator Transitions: The Case of Ca_2RuO_4 . *Phys. Rev. Lett.* **2018**, *121*, 067601.
- (18) Georgescu, A. B.; Millis, A. J. Quantifying the role of the lattice in metal-insulator phase transitions. *Communications Physics* **2022**, *5*.
- (19) Padmanabhan, H. et al. Large Exchange Coupling Between Localized Spins and Topological Bands in MnBi_2Te_4 . *Advanced Materials* **2022**, *34*, 2202841.
- (20) Nikulin, I. V.; Novojilov, M. A.; Kaul, A. R.; Mudretsova, S. N.; Kondrashov, S. V. Oxygen nonstoichiometry of $\text{NdNiO}_{3-\delta}$ and $\text{SmNiO}_{3-\delta}$. *Materials Research Bulletin* **2004**, *39*, 775–791.
- (21) Shin, Y.; Rondinelli, J. M. Pressure effects on magnetism in $\text{Ca}_2\text{Mn}_2\text{O}_5$ -type ferrites and manganites. *Physical Review B* **2020**, *102*, 104426 (2020).
- (22) Kotiuga, M.; Rabe, K. M. High-density electron doping of SmNiO_3 from first principles. *Physical Review Materials* **2019**, *3*, 115002.
- (23) Malyi, O. I.; Zunger, A. Rise and fall of Mott insulating gaps in YNiO_3 paramagnets as a reflection of symmetry breaking and remaking. *Physical Review Materials* **2023**, *7*, 1–7.
- (24) Sutton, C.; Ghiringhelli, L. M.; Yamamoto, T.; Lysogorskiy, Y.; Blumenthal, L.; Hammerschmidt, T.; Golebiowski, J. R.; Liu, X.; Ziletti, A.; Scheffler, M. Crowd-sourcing

- materials-science challenges with the NOMAD 2018 Kaggle competition. *npj Computational Materials* **2019**, *5*, 111.
- (25) Fowlie, J.; Georgescu, A. B.; Mundet, B.; del Valle, J.; Tückmantel, P. Machines for Materials and Materials for Machines: Metal-Insulator Transitions and Artificial Intelligence. *Frontiers in Physics* **2021**, *9*, 769.
- (26) Fiedler, L.; Modine, N. A.; Miller, K. D.; Cangi, A. Machine Learning the Electronic Structure of Matter across Temperatures. *Physical Review B* **2023**, *108*, 125146.
- (27) Jung, J.; Yoon, J. I.; Park, H. K.; Kim, J. Y.; Kim, H. S. Bayesian Approach in Predicting Mechanical Properties of Materials: {{Application}} to Dual Phase Steels. *Materials Science and Engineering: A* **2019**, *743*, 382–390.
- (28) Wang, H.-C.; Botti, S.; Marques, M. A. L. Predicting Stable Crystalline Compounds Using Chemical Similarity. *npj Computational Materials* **2021**, *7*, 1–9.
- (29) Ward, L.; Liu, R.; Krishna, A.; Hegde, V. I.; Agrawal, A.; Choudhary, A.; Wolverton, C. Including Crystal Structure Attributes in Machine Learning Models of Formation Energies via {{Voronoi}} Tessellations. *Physical Review B* **2017**, *96*, 24104.
- (30) Chandrasekaran, A.; Kamal, D.; Batra, R.; Kim, C.; Chen, L.; Ramprasad, R. Solving the Electronic Structure Problem with Machine Learning. *npj Computational Materials* **2019**, *5*, 22.
- (31) Ellis, J. A.; Fiedler, L.; Popoola, G. A.; Modine, N. A.; Stephens, J. A.; Thompson, A. P.; Cangi, A.; Rajamanickam, S. Accelerating Finite-Temperature {{Kohn-Sham}} Density Functional Theory with Deep Neural Networks. *Physical Review B* **2021**, *104*, 35120.
- (32) Fiedler, L.; Modine, N. A.; Schmerler, S.; Vogel, D. J.; Popoola, G. A.; Thompson, A. P.;

- Rajamanickam, S.; Cangi, A. Predicting Electronic Structures at Any Length Scale with Machine Learning. *npj Computational Materials* **2023**, *9*, 1–10.
- (33) Georgescu, A. B.; Millis, A. J.; Rondinelli, J. M. Trigonal symmetry breaking and its electronic effects in the two-dimensional dihalides MX₂ and trihalides MX₃. *Physical Review B* **2022**, *105*, 245153.
- (34) Wagner, N.; Seshadri, R.; Rondinelli, J. M. Property control from polyhedral connectivity in ABO₃ oxides. *Physical Review B* **2019**, *100*, 064101.
- (35) Rondinelli, J. M.; Spaldin, N. A. Structural effects on the spin-state transition in epitaxially strained LaCoO₃ films. *Physical Review B - Condensed Matter and Materials Physics* **2009**, *79*, 1–7.
- (36) Sterbinsky, G. E.; Nanguneri, R.; Ma, J. X.; Shi, J.; Karapetrova, E.; Woicik, J. C.; Park, H.; Kim, J. W.; Ryan, P. J. Ferromagnetism and Charge Order from a Frozen Electron Configuration in Strained Epitaxial LaCoO₃. *Physical Review Letters* **2018**, *120*, 1–6.
- (37) Kwon, J.-H.; Choi, W. S.; Kwon, Y.-k.; Jung, R.; Zuo, J.-m.; Lee, H. N.; Kim, M. Nanoscale Spin-State Ordering in LaCoO₃ Epitaxial Thin Films. *Chemistry of Materials* **2014**, *26*, 2496–2501.
- (38) Jain, A. et al. Commentary : The Materials Project : A materials genome approach to accelerating materials innovation. *APL Materials* **2013**, 011002.
- (39) Ong, S. P.; Cholia, S.; Jain, A.; Brafman, M.; Gunter, D.; Ceder, G.; Persson, K. A. The Materials Application Programming Interface (API): A simple, flexible and efficient API for materials data based on REpresentational State Transfer (REST) principles. *Computational Materials Science* **2015**, *97*, 209–215, Publisher: Elsevier BV.

- (40) Kresse, G.; Hafner, J. Ab initio molecular dynamics for liquid metals. *Phys. Rev. B* **1993**, *47*, 558–561.
- (41) Kresse, G.; Furthmüller, J. Efficiency of ab-initio total energy calculations for metals and semiconductors using a plane-wave basis set. *Computational Materials Science* **1996**, *6*, 15–50.
- (42) Kresse, G.; Furthmüller, J. Efficient iterative schemes for ab initio total-energy calculations using a plane-wave basis set. *Phys. Rev. B* **1996**, *54*, 11169–11186.
- (43) Sun, J.; Remsing, R. C.; Zhang, Y.; Sun, Z.; Ruzsinszky, A.; Peng, H.; Yang, Z.; Paul, A.; Waghmare, U.; Wu, X.; Klein, M. L.; Perdew, J. P. Accurate first-principles structures and energies of diversely bonded systems from an efficient density functional. *Nature Chemistry* **2016**, *8*, 831–836.
- (44) Varignon, J.; Bibes, M.; Zunger, A. Mott gapping in $3d ABO_3$ perovskites without Mott-Hubbard interelectronic repulsion energy U . *Phys. Rev. B* **2019**, *100*, 035119.
- (45) Karpovich, C.; Pan, E.; Jensen, Z.; Olivetti, E. Interpretable Machine Learning Enabled Inorganic Reaction Classification and Synthesis Condition Prediction. *Submitted* **2022**,
- (46) Kumar, A.; Kumari, K.; Ray, S. J.; Thakur, A. D. Graphene mediated resistive switching and thermoelectric behavior in lanthanum cobaltate. *Journal of Applied Physics* **2020**, *127*, 235103.
- (47) Shizuya, M.; Isobe, M.; Takayama-Muromachi, E. Structure and properties of the $CaFe_2O_4$ -type cobalt oxide $CaCo_2O_4$. *Journal of Solid State Chemistry* **2007**, *180*, 2550–2557.
- (48) Walters, L. N.; Tai, A. T.; Santucci, R. J.; Scully, J. R.; Rondinelli, J. M. Density Functional Theory-Based Thermodynamic Model for Stable Scale Formation in Lead-Water Systems. *The Journal of Physical Chemistry C* **2022**, *126*, 16841–16850.

TOC Graphic

